ENGINEERING TRANSACTIONS • *Engng. Trans.* • **46**, 2, 143–164, 1998
Polish Academy of Sciences • Institute of Fundamental Technological Research
10.24423/engtrans.649.1998

ROCKING-SLIDING OF A RIGID BLOCK: FRICTION INFLUENCE ON FREE MOTION

U. ANDREAUS and P. CASINI (ROMA)

Many technical problems involve contact and impact between bodies. The contact problem is locally characterized by normal and shear forces; this contact may represent different types of phenomena such as rolling, sliding, impact and shock, unilateral contact, etc. The aim of this paper is to study the "contact-impact" problem of a rigid block colliding on a frictional base, by means of a numerical simulation, and to compare numerical results with analytical responses known from the literature. Frictional contact is taken into account by means of shear forces concentrated at a discrete number of points. Attention has been paid to two-dimensional free motion of the block with three degrees of freedom. Wide ranges of block slenderness and friction angle have been investigated and numerical results have been synthesized by means of the energy reduction ratio, which accounts for contact phenomena occurring during impact.

1. INTRODUCTION

Generally speaking, for a system of bodies the fundamental equations of impulsive motion can be written as [1]:

$$\begin{aligned} m_i \Delta \mathbf{v}_{iG} &= \mathbf{f}_i^a + \mathbf{f}_i^v, \\ I_i \Delta \boldsymbol{\omega}_i &= \mathbf{m}_i^a + \mathbf{m}_i^v, \end{aligned} \tag{1.1}$$

where m_i is the mass of the single i-th body, I_i is the inertia tensor with respect to the body centroid; $\Delta \mathbf{v}_{iG}$, $\Delta \boldsymbol{\omega}_i$ are centroid and angular velocity rates, respectively, for the single body after and before the impact

$$\begin{aligned} \Delta \mathbf{v}_{iG} &= \mathbf{v}_{iG}^+ - \mathbf{v}_{iG}^-, \\ \Delta \boldsymbol{\omega}_i &= \boldsymbol{\omega}_i^+ - \boldsymbol{\omega}_i^-, \end{aligned} \tag{1.2}$$

$\mathbf{f}_i$ and $\mathbf{m}_i$ are the resultant force and moment of the impulses applied to the single body; the supercripts a and v denote active and reactive impulses, respectively. During impact active impulses are negligible with respect to reactive ones; therefore in Eqs. (1.1) we have $\mathbf{f}_i^a = \mathbf{0}$, $\mathbf{m}_i^a = \mathbf{0}$. Equations (1.2) do not generally suffice to solve the impact problem, that is to determine the velocity field after

impact, because the number of unknowns (reactive impulses and body velocities after impact) is greater than the number of equations and the problem is indeterminate; in fact, for a single body we have four vectorial unknowns $\mathbf{f}_i^v$, $\mathbf{m}_i^v$, $\Delta\mathbf{v}_{iG}$, $\Delta\boldsymbol{\omega}_i$, with respect to two vectorial equations. Instantaneous constraints at impact must be characterized from both the geometrical and mechanical point of views. Such a characterization may be (i) direct if a model is given for the contact forces during impact (deformable joint), or (ii) indirect if additional assumptions are provided about the velocity field after impact. In the latter case, degrees of freedom of the system can be limited [2], or coefficients of restitution can be quantified [3].

Thus, block-work modelization method can be classified as (i) rigid joint and (ii) deformable joint models. In the former case, a model of contact forces should be formulated at the instantaneous constraint; in the latter case, the rigid constraint assumption prevents to study the motion during impact. An alternative method is based on a variational approach which allows to determine the velocity field after impact by minimizing a suitable functional [4, 5, 6]. The problem of unilateral contact and dry friction in finite freedom dynamics is dealt with in a very general way by MOREAU [7].

2. HISTORICAL BACKGROUND

2.1. General remarks

A review on the previous research about free motion of a rigid block is given in the following; a general survey on the subject can be found in ISHIYAMA [8]. Referring to Fig. 1, let us assume that:

$$W = \mu BHg, \qquad \overline{OG} = R = \sqrt{b^2 + h^2}, \qquad b = R\sin\alpha, \qquad \alpha = \arctan(b/h),$$

where W is the deadweight of the block, having unitary depth, μ is its density mass and g is the gravitational acceleration.

2.2. Rigid contact models

Subsequent to the pioneering works of Milne and Perry, both which have appeared in 1881, the behaviour of rigid bodies during earthquake has intrigued a number of researchers for over a hundred years. These interests have been mainly motivated by the possibility of estimating the peak acceleration of earthquake excitation at sites for which no seismographic records are available. Typical examples are the contributions of researchers to the estimation of seismic intensities

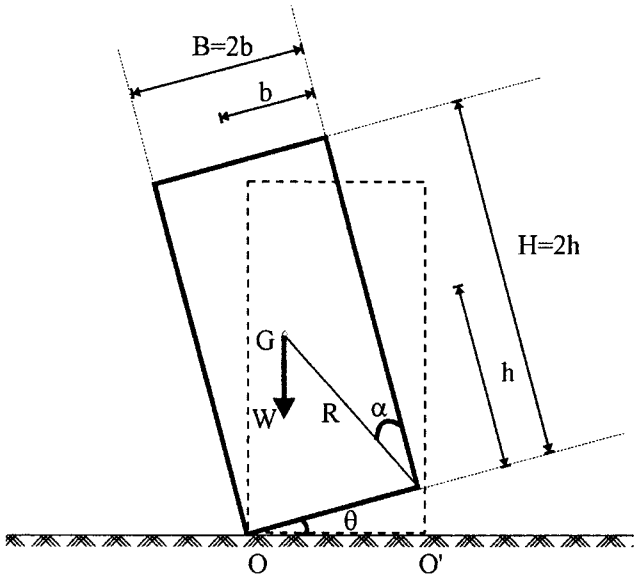

FIG. 1. Geometric characteristics and initial conditions of a rigid block.

by observing the overturning of structures attached to rigid blocks, like tombstones, columns, statues, elevated tanks.

The most common procedure used to estimate the seismic intensity at the site is to assume that the peak acceleration a was larger than the breadth/height ratio of an overturned body multiplied by the gravitational acceleration g, as represented by West's formula, firstly quoted by MILNE [9] and then reintroduced by ISHIYAMA [3, 8]:

$$a \geq g\frac{b}{h}. \tag{2.1}$$

But this criterion, Eq. (2.1), shows only the condition which initiates rocking motion and does not indicate a condition sufficient to overturn a body.

MILNE [9] is the first researcher to deal with the following problem: suppose that the column is tipped to an angle θ_0 and then allowed to fall towards the vertical. From the conservation principle of energy he proposed an estimation of the time of falling from angle θ_0 to $\theta = 0$:

$$t' = \sqrt{\frac{4\theta_0 i_0^2}{gH}}, \tag{2.2}$$

where i_0 is the radius of gyration about the point O of Fig. 1 (dot-dashed curves in Figs. 11, 12 and 13).

PERRY [10] analyzed the rocking motion of a block under the following assumptions:

- the block is rigid, has a prismatic form and a planar contact surface;
- the block alternatively rotates about the contact vertices;
- friction is sufficiently high to prevent sliding;
- complete separation is not allowed.

Thus, the equation of motion of a rocking block, whose trim is given by the angle θ, Fig. 1, is in the form of:

$$\ddot{\theta} = -\frac{m \cdot g \cdot r}{m \cdot i_0^2} \sin(\alpha - \theta), \tag{2.3}$$

where m is the mass of the block, I_0 is the moment of inertia about point O in Fig. 1. For a slender block Eq. (2.3) becomes

$$\ddot{\theta} = -\frac{mg}{I_0}(\alpha - \theta). \tag{2.4}$$

The solution of this differential equation is

$$\theta = \alpha + C_1 \mathrm{Exp}^{pt} + C_2 \mathrm{Exp}^{-pt}, \tag{2.5}$$

where

$$p = \sqrt{\frac{mgR}{I_0}},$$

C_1 and C_2 are the arbitrary constants determined by the initial conditions; when $\theta = \theta_0$, $\dot{\theta}_0 = 0$, from Eq. (2.5) Perry derived the following equation giving the time t' during which θ changes from θ_0 to 0. When pt' is small, from Eq. (2.5) we have (dotted curves in Figs. 11, 12 and 13)

$$t' = \frac{1}{p}\sqrt{\frac{2\alpha}{\alpha - \theta_0} - 2}. \tag{2.6}$$

An exact solution of Eq. (2.4) is written in the form of

$$t' = \frac{1}{p}\mathrm{Ln}\left[\frac{\alpha}{(\alpha - \theta_0)} \pm \sqrt{\left(\frac{\alpha}{(\alpha - \theta_0)}\right)^2 - 1}\right]. \tag{2.7}$$

Equation (2.7) is the same as Eq. (2.14) derived by Housner (dashed curves in Figs. 11, 12 and 13).

KIMURA and IIDA [11] analyzed the free motion of a rigid block on a rigid floor under the same assumptions as Perry. They integrated Eq. (2.3) already

introduced by Perry and obtained the time t' during which θ changes from θ_0 to zero (solid curves in Figs. 11, 12, 13):

$$t' = \frac{1}{p\sqrt{2}} \int_{\theta_0}^{0} \frac{d\theta}{\sqrt{\cos(\alpha - \theta_0) - \cos(\alpha - \theta)}}. \tag{2.8}$$

Equation (2.8) does hold also for stocky blocks. With reference to the ratio e between the values of angular velocity after and before the impact, they find, in case of rectangular block, that

$$e = \frac{3\mathrm{Cos}\, 2\alpha + 1}{4}. \tag{2.9}$$

HOUSNER [2], under the same assumptions as Perry, analysed the free rocking motion of a rigid block, Fig. 1.

As to free vibrations, the equation of motion is (as Eq. (2.3) derived by Perry)

$$I_0 \ddot{\theta} = -WR\sin(\alpha - \theta); \tag{2.10}$$

this equation represents the dynamic equilibrium in the time range between two consecutive impacts, where the first term is due to inertia force and the second one is the restoring gravitational moment.

For tall, slender columns ($\alpha \leq 20°$ following Housner), this equation becomes, as Eq. (2.4) derived by Perry,

$$\ddot{\theta} - p^2\theta = -p^2\alpha, \tag{2.11}$$

where

$$p = \sqrt{\frac{WR}{I_0}}.$$

For the initial conditions

$$\theta(t_0) = \theta_0, \qquad \dot{\theta}(t_0) = 0. \tag{2.12}$$

The solution of the above equation is

$$\theta = \alpha - (\alpha - \theta_0)\cosh pt. \tag{2.13}$$

A quarter of period, $t' = T/4$, is the time during which θ changes from θ_0 to zero:

$$t' = \frac{T}{4} = \frac{1}{p}\mathrm{arccosh}\left(\frac{1}{1 - \dfrac{\theta_0}{\alpha}}\right). \tag{2.14}$$

Equation (2.14) (dashed line in Figs. 11, 12 and 13), the same as Eq. (2.7) derived by PERRY [10], can be compared with Eq. (2.2) by Milne, Eqs. (2.6) and (2.7) by Perry, and with Eq. (2.8) by Kimura and Iida (Figs. 11, 12 and 13).

The above period has been derived under the assumption of no energy loss, but actually the energy dissipates at each impact between the base of the body to the floor. If we assume the conservation of momentum about O', Fig. 1, we have the ratio e of the values of angular velocity after and before the impact (coefficient of restitution of angular velocities), as Eq. (2.9) derived by KIMURA and IIDA [11]:

$$e = \frac{\dot{\theta}^+}{\dot{\theta}^-} = \frac{2\left(\frac{h^2}{b^2}\right) - 1}{2\left(1 + \frac{h^2}{b^2}\right)}. \tag{2.15}$$

This coefficient depends only upon the block slenderness and tends to unity (perfectly elastic impact) as the slenderness H/B increases.

The results given by Housner for the free motion of a rigid block can be synthesized by the following observations.

The motion of the block can be described as a repetition of the following cycle, which exhibits four steps:

(i) The block from initial conditions $\theta = \theta_0 = 0$, achieves, rotating about the vertex O, the rest position $\theta = 0$ with angular velocity $\dot{\theta}_1$ at time t_1.

(ii) The block initiates rotating about the vertex O', with angular velocity $\dot{\theta}_2 < \dot{\theta}_1$, arriving at $\theta_2 < \theta_0$ at time t_2 with $(t_2 - t_1) < t_1$.

(iii) The block rotates about vertex O', with initial angular velocity equal to zero and initial rotation equal to θ_2, going to rest with angular velocity $\dot{\theta}_3$ at time t_3, with $(t_3 - t_2) < (t_2 - t_1)$.

(iv) The block rotates once more about point O, with initial angular velocity $\dot{\theta}_4 < \dot{\theta}_3$, arriving at $\theta_4 < \theta_2$ at time t_4, with $(t_4 - t_3) < (t_3 - t_2)$.

On the basis of the previous observations, it can be inferred that the block motion is damped with a decreasing period T. In more detail, T is the duration of the cycle constituted by the above mentioned four steps; T can be interpreted as a pseudo-period, because it decreases from cycle to cycle. Thus the quantity t', which is the time used by the block to perform step (i) of a single cycle, can be determined as a quarter of the pseudo-period T, and hence defined the "quarter-period".

Furthermore, Housner gives, at the n-th impact, the amplitude and the half-period $T/2$:

$$\theta_n = \alpha\left\{1 - \sqrt{\mathrm{Exp}^{2n}\left[1 - \left(1 - \frac{\theta_0}{\alpha}\right)^2\right]}\right\}, \tag{2.16}$$

$$\frac{T_n}{2} = \frac{2}{n}\mathrm{Tanh}^{-1}\sqrt{\mathrm{Exp}^{2n}\left[1-\left(1-\frac{\theta_0}{\alpha}\right)^2\right]}. \tag{2.17}$$

GIANNINI [12] assumes that one of the two contact points during impact is located at distance ηb from the edge ($0 < \eta < 1$); therefore the energy reduction ratio is

$$r = \left[\frac{4\left(\frac{h}{b}\right)^2 - 2 + 3\eta}{4\left(\frac{h}{b}\right)^2 + 4 - 3\eta}\right]^2, \tag{2.18}$$

which for $\eta = 0$ coincides with the value given by Housner, whereas for $\eta \to 1$ it tends to 1 (perfectly elastic impact).

The work by ISHIYAMA [3] slightly differs from Housner's approach. He considers possible motion modes of a rigid block, namely rest, slide, rotation, slide rotation, translation jump, rotation jump. The Author writes down for each motion mode the dynamic equations including friction as well as the continuity conditions between them. As far as the impact is concerned, he defines the coefficient of restitution in terms of velocities tangential to the contact surface, in addition to the coefficient of restitution in terms of angular velocities.

LIPSCOMBE [13] extended Housner's model taking into account for the block the possibility of bouncing on the base after impact. Let us consider the case of a rectangular block which, prior to impact, is rotating about edge O, as in Fig. 1. At the instant that edge O' impacts on the foundation, the block lifts off the foundation at edge O; but, if bouncing occurs, then edge O' also lifts off. Note that while the block is airborne, it is subjected to gravity acceleration only, therefore its angular velocity remains constant between two impacts. The same phenomenon has been exhibited in a number of numerical simulations, Fig. 14. In more detail, Lipscombe takes into account the possibility of bouncing on the base after impact, by means of a coefficient of restitution ε in terms of velocities orthogonal to the contact surface. He assumes no sliding between the block and the base. The author gives the following relation e and ε:

$$e = \frac{\dot{\theta}^+}{\dot{\theta}^-} = \frac{2h^2 - b^2 - 3b^2\varepsilon}{2(h^2 + b^2)}. \tag{2.19}$$

This model shows that if the slenderness is small enough, bouncing has a negligible influence on the motion.

IYENGAR and ROY [14] investigate the planar rocking of a prismatic rectangular rigid block and consider the full nonlinear system without the assumption of slenderness and consequent piecewise linear property, under the action of base acceleration.

2.3. Deformable contact models

The basic joint model proposed by CUNDALL [15] captures several of the features which are representative of the physical response of joints. In the normal direction, the stress-displacements relation is assumed to be linear; there is also a limiting tensile strength for the joint. In shear, the response is controlled by a constant shear stiffness; the shear stress is limited by a combination of cohesive and frictional strength.

PSYCHARIS and JENNINGS [16] proposed a deformable joint model consisting of an infinite number of independent linearly elastic springs; it is assumed that springs take no tension; they studied either free and forced motion of a rigid block on this foundation. No sliding is allowed between the block and the base; therefore the block exhibits two degrees of freedom: lift-off and rocking; unfortunately, this assumption may not be valid for stocky blocks. The Authors consider an equivalent model consisting of two springs at the vertices of the block.

ANGOTTI and TONI [17] study the dynamic behaviour of a rigid block with three degrees of freedom supported by a no-tension spring foundation. The single independent spring exhibits a multi-linear behaviour in compression; two-linear springs simulate lateral resistance of soil.

ANGOTTI, CHIOSTRINI and TONI [18] refined the above mentioned model by considering viscous damping; they analysed the behaviour of a two-block system, where the joint between blocks is rigid and a no-tension foundation simulates soil-structure interaction. The upper block can exhibit only rocking motion and complete separation is accounted for as an ultimate state.

A distinct element model was proposed by one of the Authors, which was based on piece-wise linear coupled normal and shear forces at a discrete number of contact points [19] for cyclic analysis of rigid block–work structures; furthermore, a dynamic analysis of deformable blocks was performed [20] where joint behaviour was simulated by means of the above mentioned model. Finally seismic analysis of rigid block on hysteretic foundation was worked out by ANDREAUS [21].

ANDREAUS and NISTICÒ [22] proposed an analytical-numerical model of a distinct element which is suitable to analyse contact-impact problems between interacting rigid bodies, Fig. 2. Deformability is limited at joint surfaces and is taken into account by means of contact forces concentrated at a discrete number of physical contacts. Refined analytical stress-strain relations in normal and tangential directions with respect to the contact surfaces are formulated which allow to account for (i) uplifting and hysteretic damping in normal direction, (ii) coupling between shear strength and compression force, friction dissipation and cumulating damage in tangential direction.

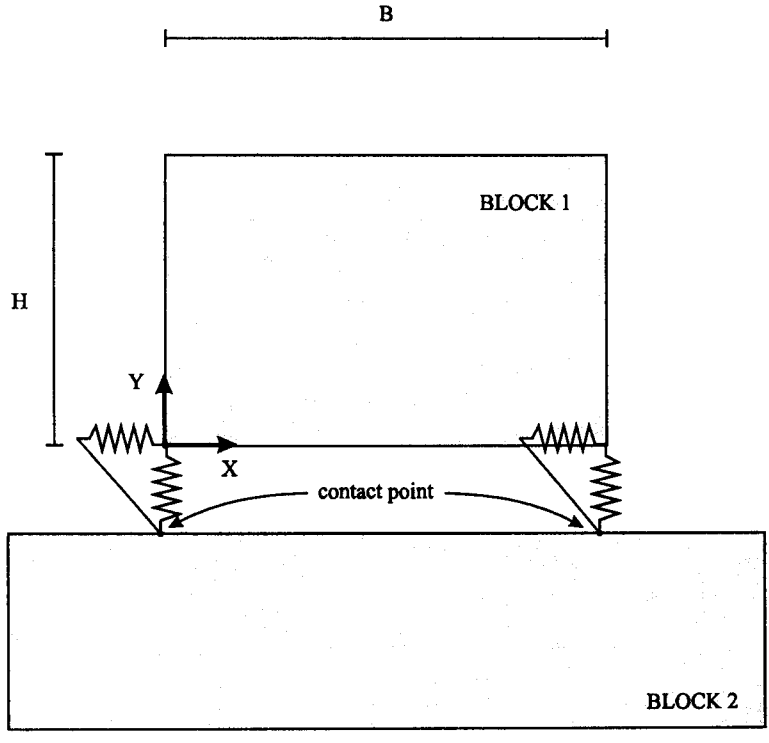

FIG. 2. Hysteretic model of contact forces between blocks [22].

In more detail the contact behaviour in normal direction is defined as follows:

$$
\begin{aligned}
n &= N + (n_0 - N)e^{-\beta\frac{d-d_0}{D-d}}, \\
n &= 0 \qquad (d \geq 0),
\end{aligned}
\tag{2.20}
$$

where n and n_0 are the contact forces at the current and previous time step, respectively, β is a model parameter used for describing the rate at which the contact force within a hysteresis loop approaches the corresponding (lower or upper) envelope curve which has the following form:

$$
N = A\frac{D}{D-d}d, \tag{2.21}
$$

where d is the contact closure, N is the compressive force, A the initial stiffness, D the limit overlap. There is also a limiting compressive strength, $\overline{N}$, for the contact if the compressive strength is exceeded, then local failure occurs and contact is lost. Lower and upper envelope curves are characterized by different values, A_l and A_u, of parameter A.

The shear strength at the single contact due to macro-asperities along the interfaces is defined as a multi-state variable law

$$T = n\mu \left[1 - e^{(-\delta|s-s_R|)/b}\right] \frac{\dot{s}}{|\dot{s}|}, \qquad \mu = \operatorname{Tan}(\varphi_1 + \varphi_2). \tag{2.22}$$

where T = contact shear force, s = relative tangential displacement, i.e. current slip, s_R = slip at the last reversal point, $\dot{s}$ = relative tangential speed (slip rate), φ_1 = current value of incremental angle due to macro-asperities, φ_2 = current value of residual angle due to micro-asperities, $\varphi_1 + \varphi_2$ = peak value of friction angle, δ = nondimensional parameter governing the slope of the shear strength curve.

Angle φ_1 depends on normal force, normal force rate, cumulative relative displacement s_C and relative speed $|\dot{s}|$ as the following law:

$$\varphi_1 = \varphi_0 \exp -cC_nC_s, \tag{2.23}$$

with φ_0 = initial value of incremental angle φ_1,

$$n < 0, \qquad \overline{N} < 0, \qquad n \geq \overline{N}, \qquad \overline{\dot{n}} < 0;$$

$$C_n = \left(\frac{n}{\overline{N} - n}\right)^{h_n}, \qquad \begin{cases} \dot{n} \geq \overline{\dot{n}} \Rightarrow h_n = c_n, \\ \dot{n} < \overline{\dot{n}} \Rightarrow h_n = c_n \dfrac{\dot{n}}{\overline{\dot{n}}}, \end{cases}$$

$$s_C = \int_0^t |\dot{s}|\, d\tau, \qquad \overline{\dot{s}} > 0;$$

$$C_s = \left(\frac{s_C}{\overline{s}_C - s_C}\right)^{h_s}, \qquad \begin{cases} |\dot{s}| \leq \overline{\dot{s}} \Rightarrow h_s = c_s, \\ |\dot{s}| > \overline{\dot{s}} \Rightarrow h_s = c_s \dfrac{|\dot{s}|}{\overline{\dot{s}}}, \end{cases}$$

$\overline{s}_C$ is the yield value of cumulative slip, such that, if exceeded, shear damage stops and only residual friction is exhibited by the joint; $\overline{\dot{n}}$, $\overline{\dot{s}}$ are yield values of compression and absolute slip rates respectively such that, if exceeded, load-rate effect is exhibited by the contact, simulating the influence of impact velocity on shear response of the joint; c is a nondimensional parameter governing the slope of the current value of incremental angle due to macro-asperities; c_n and c_s are nondimensional parameter tuning, respectively, the compression and slip rates.

Moreover, the current value of residual angle φ_2 deteriorates according to the following law ("aquaplane" effect):

$$\varphi_2 = \varphi_r \exp -|\dot{s}|/\tilde{\dot{s}}, \qquad \tilde{\dot{s}} \geq 0, \tag{2.24}$$

φ_r = initial value of residual angle φ_2, $\tilde{\dot{s}}$ = suitable reference value of slip rate.

Parameters φ_0, φ_r, $\bar{s}_C$, $\bar{\dot{n}}$, $\bar{\dot{s}}$, $\tilde{\dot{s}}$ are to be identified on experimental basis. For more details, concerning the experimental identification of the above mentioned parameters, the reader may refer to the fundamental and extended works by BARTON and CHOUBEY [23], BANDIS, LUMSDEN and BARTON [24], BARTON, BANDIS and BAKHTAR [25]; and to BANDIS, LUMSDEN and BAKHTAR [26] as far as the size effect is concerned.

2.4. Variational approach models

SINOPOLI [4] studies the dynamics and the impact of a rigid block in order to evaluate the influence of friction and to analyse the motion after impact either for zero and infinite friction. The unique velocity field after impact has been determined by means of a refined version of the Gauss minimum constriction principle [27] due to Robin. For zero friction, the coefficient of restitution in terms of angular velocities depends on slenderness according to

$$
\begin{aligned}
& r = \frac{\dot{\theta}^{+2}}{\dot{\theta}^{-2}} = \left[\frac{H^2 - 2B^2}{4B^2 + H^2}\right]^2, \qquad && \frac{H}{B} > \sqrt{2}, \\
& r = 0, && \frac{H}{B} \leq \sqrt{2}.
\end{aligned} \tag{2.25}
$$

For infinite friction, the same results as those given by Housner are obtained

$$
r = \frac{\dot{\theta}^{+2}}{\dot{\theta}^{-2}} = \left[\frac{2H^2 - B^2}{2(B^2 + H^2)}\right]^2, \qquad \frac{H}{B} > \frac{\sqrt{2}}{2}. \tag{2.26}
$$

3. COMPARISON BETWEEN ANALYTICAL AND NUMERICAL RESULTS

3.1. General results

On the basis of the model proposed by ANDREAUS and NISTICÒ [22], several sample applications have been worked out as far as free motion of rigid blocks in two dimensions is concerned; initial conditions $\theta = \theta_0$, $\dot{\theta}_0 = 0$ have been assumed. No size effect has been revealed in all cases dealt with. Rectangular blocks have been considered having different slenderness, breadth $B = 0.12\,\mathrm{m}$, height $H = 0.24 \div 1.20\,\mathrm{m}$, thickness $0.06\,\mathrm{m}$, and mass density $2700\,\mathrm{Kg/m^3}$.

3.2. Finite friction influence on free motion

Influence of friction on the dynamic behaviour of block-work structures is undoubtedly a very interesting subject, but in Authors' opinion it is still an open problem. Influence of friction on free response in terms of energy reduction ratio r has been evaluated after the first impact.

Figure 3 presents the coefficient of restitution r versus the initial value of the residual friction angle φ_r, according to the model proposed by ANDREAUS and NISTICÒ [22]; the slenderness range is $\lambda = H/B = 2.0 \div 10.0$ and the initial condition is $\theta_0/\alpha = 0.5$. It is worth noting that the curves in Fig. 3 exhibit a minimum. Characteristic friction angle at which minimum occurs is denoted by the symbol $\hat{\varphi}_r$. If kinetic energy of the block before the first impact K^- is presented versus friction angle φ_r, a minimum can be observed which increases as slenderness decreases, Fig. 4. The friction angle at which minimum is attained is called "critical" and denoted by the symbol φ_r^*; the kinetic energy has been normalized with respect to the energy at infinite friction.

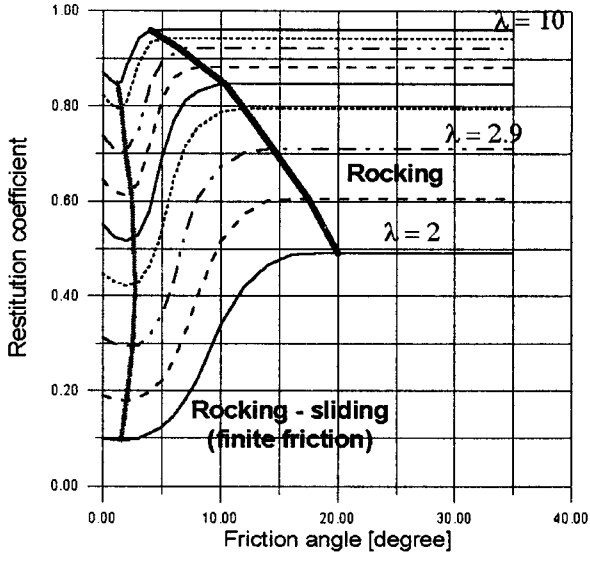

FIG. 3. Separation curves between different modes of motion in terms of friction.

For very high friction ($\varphi_r \geq \varphi_r^y$) the coefficient of restitution attains a yield limit which coincides with that derived by KIMURA and IIDA [11], Eq. (2.9), as well as with that derived by HOUSNER [2], Eq. (2.15). In Fig. 3 light and heavy solid lines are minima and maxima *loci*, respectively. In more detail, light solid line represents the *locus* of characteristic friction angles $\hat{\varphi}_r$ and heavy solid line represents the *locus* of yield angles φ_r^y (rocking).

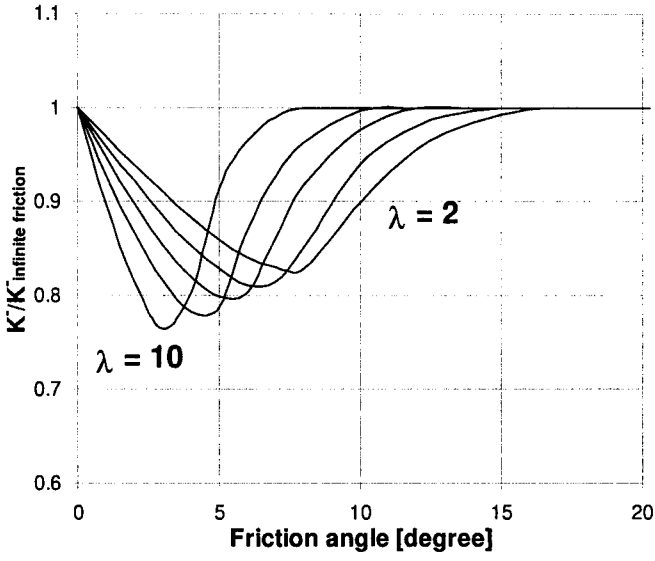

FIG. 4. Dependence of the kinetic energy before first impact on friction.

The motion of the block exhibited subsequent impacts till rest; the following observations can be made in all cases dealt with, Fig. 5.

(i) For zero friction the block centroid exhibits no slide, according to the conservation principle of momentum; therefore the vertex which has coincided with the first contact point (point O, Fig. 1) exhibits a slide equal to $\Delta s = b[(1 - \mathrm{Cos}\,\theta_0) + \lambda \mathrm{Sin}\,\theta_0]$; for a very wide range of slenderness (from 0.5 to ∞)

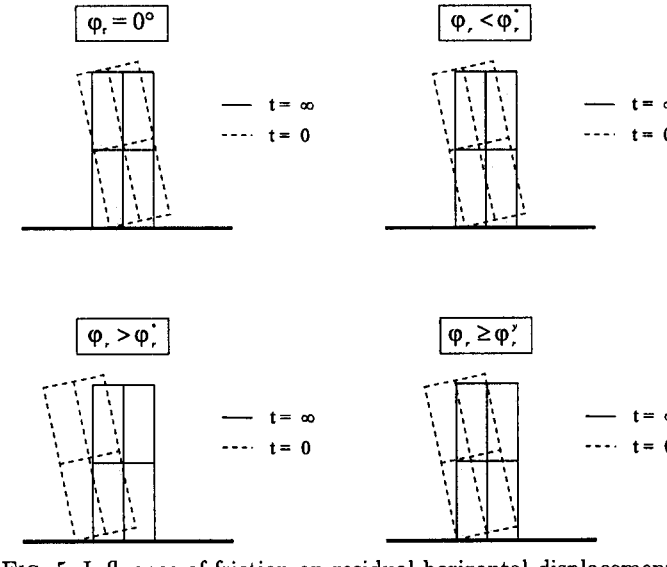

FIG. 5. Influence of friction on residual horizontal displacement.

Δs is a very flat function of λ, inasmuch as we have $\alpha = \mathrm{ArcTan}\,\lambda^{-1}$ and a fixed ratio θ_0/α has been taken as initial condition. The direction of slide Δs is such to satisfy the above mentioned conservation principle.

(ii) For friction range $0 \leq \varphi_{<}\varphi_r^*$ the vertex which has coincided with the first contact point exhibits, during the first quarter period, a slide whose direction is the same as the slide for zero friction at item (i); afterwards the vertex coinciding with the second contact point (point O' in Fig. 1) exhibits a slide in the opposite direction and of smaller magnitude with respect to that exhibited by point O; therefore, the vertex O exhibits a slide in the same direction with respect to that for zero friction at item (i) and of decreasing magnitude.

(iii) At critical friction angle φ_r^*, the vertex which has coincided with the first contact point exhibits, during the first quarter period, a slide whose direction is the same as the slide for zero friction at item (i); afterwards the vertex coinciding with the second contact point (point O' in Fig. 1) exhibits a slide in the opposite direction with respect to that exhibited by point O and of equal magnitude; therefore, the vertex O, at the end of motion, goes back to the initial position.

(iv) For friction range $\varphi_r^* \leq \varphi_r \leq \varphi_r^y$, the vertex which has coincided with the first contact point exhibits, during the first quarter period, a slide in the same direction with respect to that one at item (i); afterwards the vertex coinciding with the second contact point (point O' in Fig. 1) exhibits a slide in the opposite direction and of larger magnitude with respect to that exhibited by point O; therefore, the vertex O, at the end of motion, exhibits a slide in the opposite direction with respect to that for zero friction at item (i) and of magnitude which attains a maximum and then tends to zero, Figs. 6, 7.

(v) For friction range $\varphi_r^y \leq \varphi_r < \infty$, the vertices O and O' exhibit negligible slides and, in the case of slender blocks, assumptions made by PERRY [10] and HOUSNER [2] are fulfilled.

For slender blocks ($\lambda \geq 5$) slide of items (i) and (iv) is combined with rocking, Fig. 8. It is worth noting that the critical friction angle φ_r^* depends on the ratio θ_0/α; in more detail, φ_r^* corresponds to the first zero points of the curves in Fig. 7, and φ_r^* decreases as the ratio θ_0/α increases, Fig. 7.

Moreover, when $\theta_0/\alpha \approx 1$, the yield value φ_r^y of the friction angle depends only upon the block slenderness according to $\mathrm{Tan}\,(\varphi_r^y) = \lambda^{-1}$; thus, slide is negligible for $\mathrm{Tan}\,(\varphi_r) \geq \lambda^{-1}$. This is in agreement with the results of Omori [1881] quoted by ISHIYAMA [8]: he compared the inertia force to overturn (incipient rocking) the body given by West's formula, Eq. (2.1), with the friction force and concluded that the body will slide instead of overturn if λ^{-1} is greater than the friction coefficient $\mu = \mathrm{Tan}\,(\varphi_r)$;

Furthermore, the coefficient of restitution r has been reported versus slenderness λ for a friction range $\varphi_r = 0 \div 14°$ and ∞, Fig. 9. The two limit curves

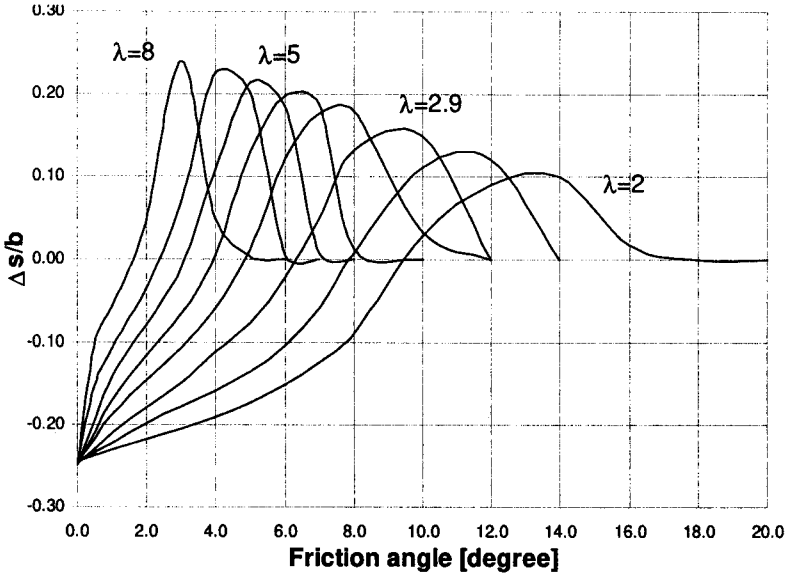

FIG. 6. Influence of friction on residual horizontal displacement: different slenderness ratios at $\theta_0/\alpha = 1/2$.

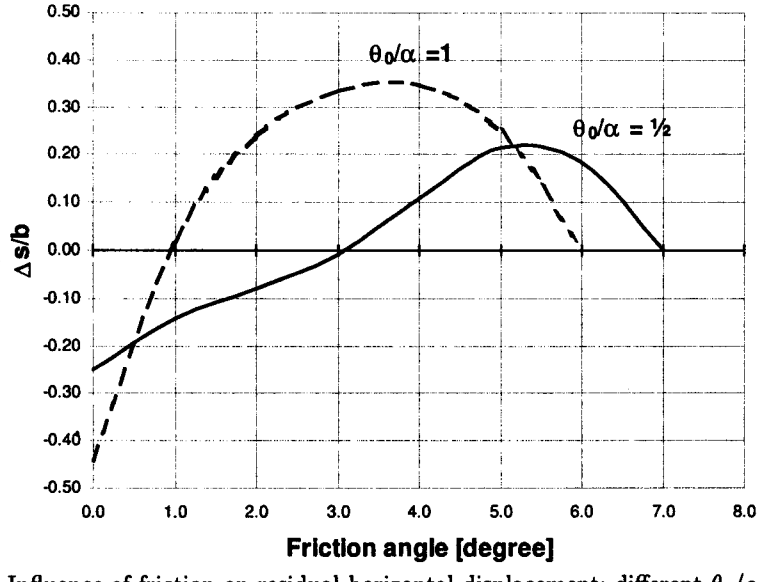

FIG. 7. Influence of friction on residual horizontal displacement: different θ_0/α ratios at $\lambda = 5.0$.

refer to zero friction [4], Eq. (2.25) (light solid line) and infinite friction (heavy solid line), Eq. (2.9) [11] or Eq. (2.15) [2]. It is worth noting that for intermediate friction angles we have curves located between the two limit curves; these curves

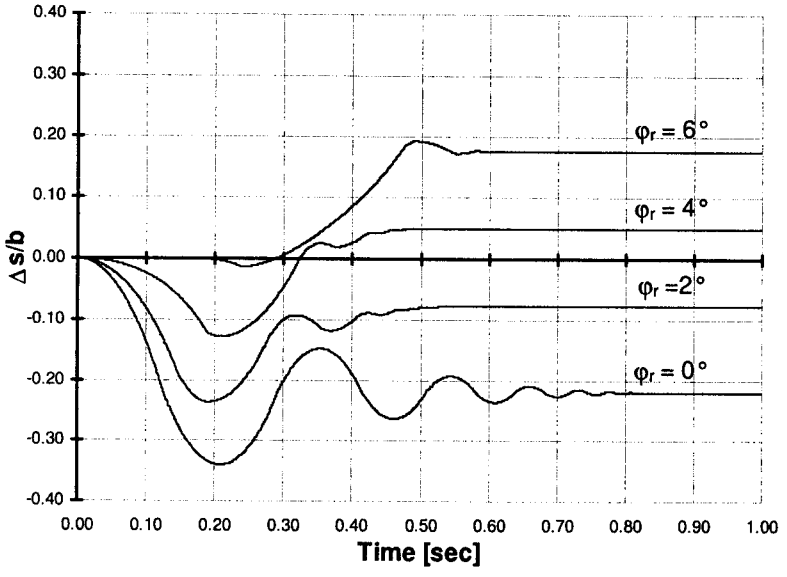

FIG. 8. Time-histories of residual horizontal displacement.

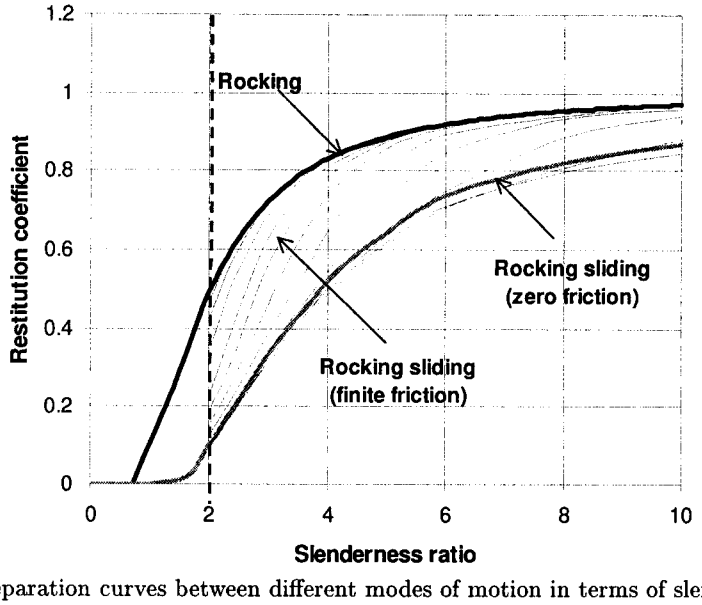

FIG. 9. Separation curves between different modes of motion in terms of slenderness.

tend to the heavy solid line for increasing friction angle; the curves corresponding to low values of friction angle intersect the light solid line; this is because the coefficient of restitution attains a minimum at the characteristic friction angle $\hat{\varphi}_r$, and it is greater than zero. Moreover, the limit curves do not depend upon the ratio θ_0/α, according with Eqs. (2.25) and (2.15).

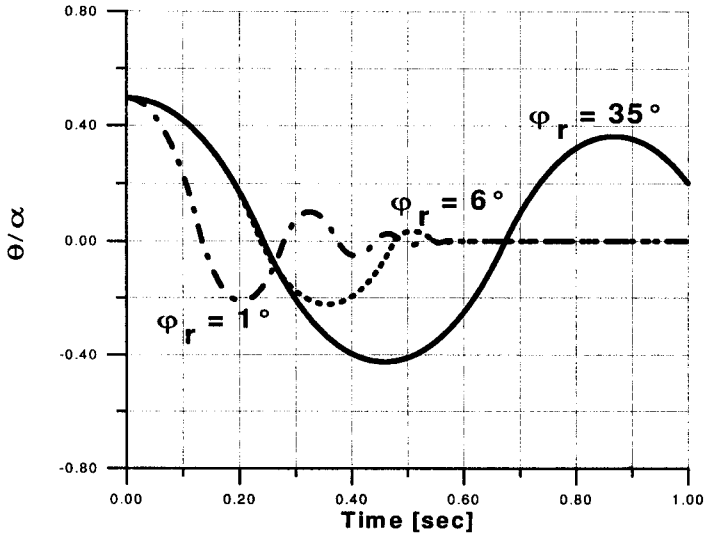

FIG. 10. Time-history of the rotation.

Referring to a block of slenderness $\lambda = 5.0$ and with initial conditions $\theta = \alpha/2$, $\dot{\theta}_0 = 0$, Fig. 10 reports the time-history of the rotation. The time-history has been evaluated for the following values of the friction angle: $\varphi_r = 0°$ (dashed line), 1° (dot-dashed lines), 6° (dotted lines) 35° (solid lines); in this case it is found that $\varphi_r^* \cong 3°$, $\varphi_r^y \cong 11°$.

3.3. Free motion at infinite friction

A comparison has been performed between the numerical solution of the exact equation, Eq. (2.3), derived by KIMURA and IIDA [11], and the analytical solutions of the approximate equation, Eq. (2.4), derived by MILNE [9] and PERRY [10]. Figures 11, 12 and 13 report the quarter period $T/4$ versus the ratio θ_0/α for different block slendernesses. Milne's approximation underestimates the quarter period for high (Fig. 11) and overestimates it for low (Fig. 13) slendernesses, whereas Milne's approximation is sufficiently accurate for slenderness $\lambda \approx 1$ and for $\theta_0/\alpha \leq 0.3$, Fig. 12. From high slendernesses up to $\lambda \approx 1$, the numerical solution of the exact equation, Eq. (2.3) and the analytical solution, Eqs. (2.13) or (2.7), of the approximate equation practically coincide. For slendernesses greater than 1 and for low values of θ_0/α, the analytical solution of the approximate equation underestimates $T/4$. In Figs. 11, 12 and 13 the analytical solutions presented in the literature have been compared with the numerical results found by the authors by means of the numerical procedure proposed in [22] (squared dots).

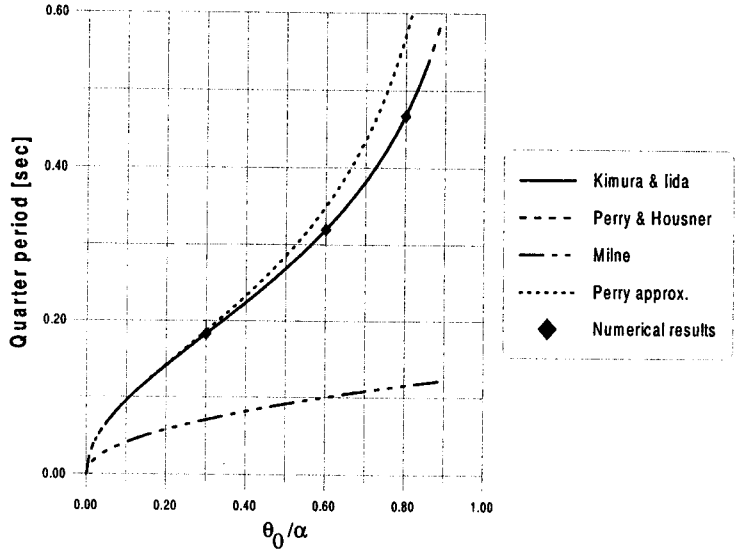

FIG. 11. Influence of initial condition on quarter period: $\lambda = 5.0$.

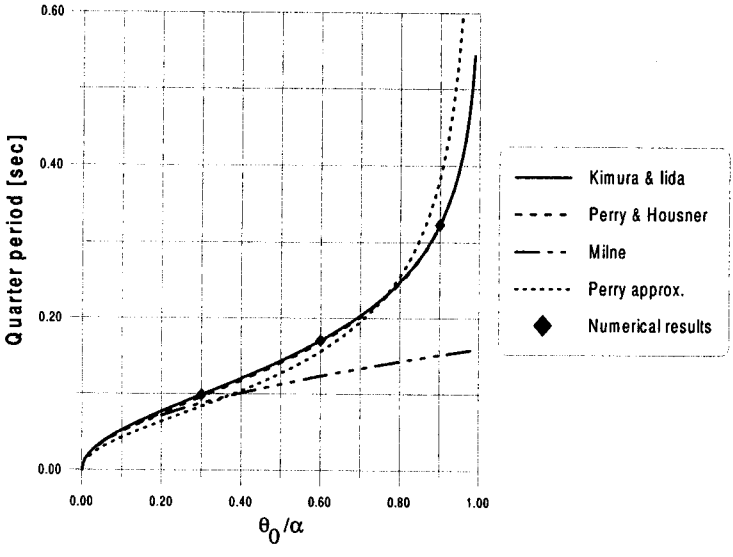

FIG. 12. Influence of initial condition on quarter period: $\lambda = 1$.

At the end, for some values of slenderness ($\lambda = 5$, 3.6, 2.9, 2) and for friction angles larger than the yield value φ_r^y, the time-histories of rotations exactly coincide with Housner's solution, Eqs. (2.16) and (2.17).

For low slendernesses ($\lambda \leq \sqrt{2}/2$), the phenomenon of bouncing has been observed: the angular velocity exhibits rapidly damped oscillations during the impact of a vertex on the basis, Fig. 14, as already observed by LIPSCOMBE [13].

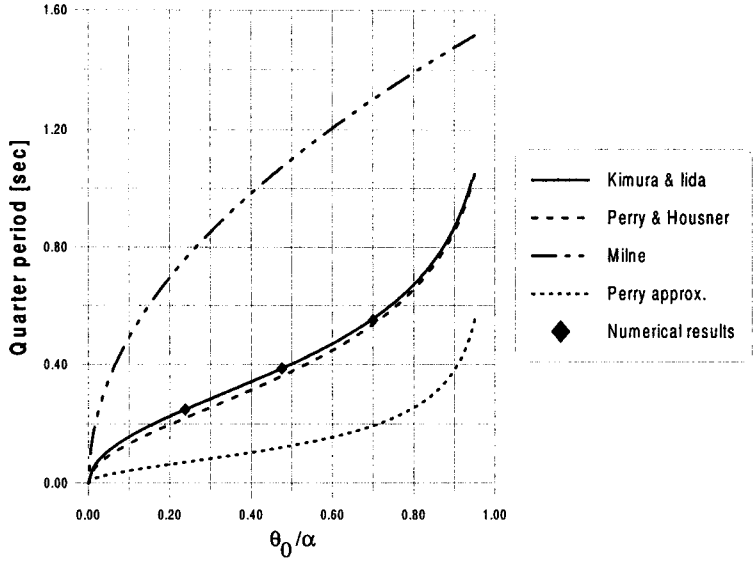

FIG. 13. Influence of initial condition on quarter period: $\lambda = 0.10$.

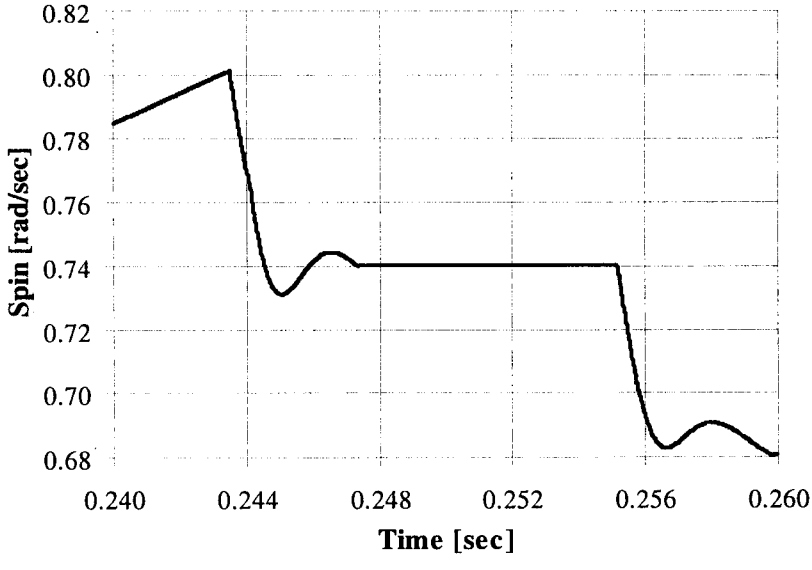

FIG. 14. Magnification of bouncing effect during impact in terms of spin.

The parameters of the model in Fig. 2 have been identified by means of the procedure outlined in [22]; for example, values used for the block of slenderness 5 are: $\overline{N} = 1. \times 10^{+6}$ KN, $\beta_u = \beta_l = 5.$, $\overline{\dot{n}} = \overline{\dot{s}} = \tilde{\dot{s}} = \infty$, $\overline{s}_C = 1$ m; $D = 2. \times 10^{-4}$ m, $A_l = 1. \times 10^{+4}$ KN/m, $A_u = 3703.$ KN/m; $\delta = 0.12 \times 10^{+4}$, $\varphi_0 = 0.°$, $c = 1.$, $c_n = c_s = 5$.

4. Conclusions

Free motion of a rigid rectangular block on a frictional foundation has been studied under initial conditions of a given rotation angle about a vertex and zero angular velocity, by means of a numerical simulation.

Wide ranges of block slenderness and friction angle have been explored in order to investigate the dynamic behaviour of the system under examination before and after impact. In more detail, the so-called "pseudo-period" versus motion amplitude, and the coefficient of restitution versus block slenderness and versus friction angle have been considered. A very good agreement between the numerical and theoretical results has been shown in the case where an analytical solution is available, i.e. for zero and infinite friction.

As far as intermediate values of friction angle are concerned, numerical simulation has allowed to reveal the dependence of the energy reduction upon block slenderness and friction angle; moreover, the existence of a characteristic value $\hat{\varphi}_r$ of the friction angle has been detected for each slenderness, which minimizes the coefficient of restitution versus friction angle. Furthermore, the existence of a critical value φ_r^* of the friction angle, for a given block slenderness, has been detected, such that magnitude of residual slide (at rest) of the first contact point is zero. It is worth noting that kinetic energy of the block before impact attains a minimum at the critical value φ_r^* of the friction angle.

Finally, for free motion sliding is negligible during rocking depending on the relative amount of friction angle φ_r of the contact and slenderness λ of the block. Experimental analysis of the rocking rigid block with $\lambda = 2$ and different values of friction coefficient has been conducted in [28] under horizontal harmonic excitation characterized by various frequencies and amplitudes. It was noted that the rocking onset depends on friction, but that when rocking occurs, the trajectory does not depend on the friction.

References

1. K. Muto, H. Takase, K. Horikoshi and H. Ueno, *3-D nonlinear dynamic analysis of stacked blocks*, Proc. 2-nd Special Conf. on "Dynamic response of structures: experimentation, observation, prediction and control", Mech. Div., ASCE, Atalanta, Georgia, 917–930, 1981.

2. G.W. Housner, *The behaviour of inverted pendulum structures during earthquakes*, Bull. Seism. Soc. of Amer., **53**, 2, 403–417, 1963.

3. Y. Ishiyama, *Motions of rigid bodies and criteria for overturning by earthquake excitations*, Earthquake Engrg. Struct. Dyn., **10**, 635–650, 1982.

4. A. Sinopoli, *Dynamics and impact in a system with unilateral constraints. The relevance of dry friction*, Meccanica, **22**, 4, 210–215, 1987.

5. G. AUGUSTI and A. SINOPOLI, *Modelling the dynamics of large block structures*, Meccanica, **27**, 3, 195–211, 1992.

6. A. SINOPOLI and V. SEPE, *Coupled motion in the dynamic analysis of a three block structure*, Appl. Mech. Rev., **46**, 11, Part 2, 186–197, 1993.

7. J.J. MOREAU, *Unilateral contact and dry friction in finite friction dynamics*, [in:] Non Smooth Mechanics and Applications, J.J. MOREAU and P.D. PANAGIOTOPOULOS [Eds.], CISM Courses and Lectures, 302, Springer-Verlag, 1–82, 1988.

8. Y. ISHIYAMA, *Review and discussion on overturning of bodies by earthquake motion*, Rep. Build. Res. Inst., Min. of Constr., Japan, June 1980.

9. J. MILNE, *Experiments in observational seismology*,. Trans. of the Seism. Soc. of Japan, 3, 12–24, 1881.

10. J. PERRY, *Note on the rocking of a column*, Trans. of the Seism. Soc. of Japan, 3, 103–106, 1881.

11. H. KIMURA and K. IIDA, *On rocking of rectangular columns* (I) [in Japanese], Zishin (J. of the Seism. Soc. of Japan), **6**, 3, 125–149, 1934; H. KIMURA and K. IIDA, *On rocking of rectangular columns* (II) [in Japanese], Zishin (J. of the Seism. Soc. of Japan), **6**, 4, 165–212, 1934.

12. R. GIANNINI, *Considerazioni sulla modellazione numerica di sistemi di blocchi rigidi sovrapposti* [in Italian], Proc. Conf. on "Stato dell'arte in Italia sulla meccanica delle murature", Rome, 677–685, 1985.

13. P.R. LIPSCOMBE, *Dynamics of rigid block structures*, Dissertation submitted to the University of Cambridge for the degree of Doctor of Philosophy, 1990.

14. R.N. IYENGAR and D. ROY, *Nonlinear dynamics of a rigid block on a rigid base*, J. Appl. Mech., **63**, 55, 55–61, 1996.

15. P. CUNDALL, *A computer model for simulating progressive large-scale movements of blocky rock system*, Proc. of the Symposium of the Int. Soc. of Rock Mechanics, Nancy, France, Vol. I, 132–150, 1971.

16. I.N. PSYCHARIS and P.C. JENNINGS, *Rocking of slender rigid bodies allowed to uplift*, Earthquake Engrg. Struct. Dyn., **11**, 1, 57–76, 1983.

17. F. ANGOTTI and P. TONI, *Oscillazioni non lineari di corpi rigidi su semispazi elastici monolaterali* [in Italian], Proc. 6-th Conf. AIMeTA, 134–143, Genoa 1982.

18. F. ANGOTTI, S. CHIOSTRINI and P. TONI, *Analisi dinamica e sismica di strutture a deformabilità limitata su suolo monolaterale* [in Italian], Proc. 7-th Conf. AIMeTA, **5**, 409–420, Trieste 1984.

19. U. ANDREAUS, *A frictional model for sliding of jointed blocks*, Proc. ICCLEM (Asia), 1, 249–254, Chongqing, China 1989.

20. U. ANDREAUS, *Dynamic analysis of deformable block-work structures*, Proc. 9-th Conf. on Earthquake Engineering, **7-C**, 61–70, Moscow 1990.

21. U. ANDREAUS, *Sliding-uplifting response of rigid blocks to base excitation*, Earthquake Engrg. Struct. Dyn., **19**, 1181–1196, 1990.

22. U. ANDREAUS and N. NISTICÒ, *An analytical-numerical model for contact-impact problems: theory and implementation in a 2-D distinct element algorithm*, Computer Modelling and Simulation in Engineering, **3**, 2, 98–110, 1998.

23. N.C. BARTON and V. CHOUBEY, *The shear strength of rock joints in theory and practice*, Rock Mech., **10**, 1–54, 1977.

24. S.C. BANDIS, A.C. LUMSDEN and N.C. BARTON, *Fundamentals of rock joint deformation*, Int. J. Min. Sci. and Geomech. Abstr., **20**, 6, 249–268, 1983.

25. N.C. BARTON, S.C. BANDIS and K. BAKHTAR, *Strength, deformation and conductivity coupling of rock joints*, Int. J. Min. Sci. and Geomech. Abstr., **22**, 3, 121–140, 1985.

26. S.C. BANDIS, A.C. LUMSDEN and N.C. BARTON, *Experimental studies of scale effects on the shear behaviour of rock joints*, Int. J. Min. Sci. and Geomech. Abstr., **18**, 1, 1–21, 1981.

27. T. LEVI CIVITA and U. AMALDI, *Lezioni di Meccanica Razionale* [in Italian], Zanichelli 1927.

28. M. RAOUS, *Experimental analysis of the rocking of a rigid block*, 3rd Pan-American Congress of Applied Mechanics (PACAM III), 61–64, Sao Paolo 1993.

DIPARTIMENTO DI INGEGNERIA STRUTTURALE E GEOTECNICA,
FACOLTÀ DI INGEGNERIA, UNIVERSITÀ DEGLI STUDI DI ROMA "LA SAPIENZA"
Via Eudossiana 18, 00184 Roma, Italy.

Received January 5, 1998; new version April 21, 1998.